Pergamon

Int. J. Solids Structures Vol. 32, No. 22, pp. 3359–3372, 1995
Copyright © 1995 Elsevier Science Ltd
Printed in Great Britain. All rights reserved
0020-7683/95 $9.50 + .00

0020-7683(94)00305-X

MICROMECHANICAL MODELLING OF TENSILE RESPONSE OF ELASTIC–BRITTLE MATERIALS

XI-QIAO FENG and SHOU-WEN YU†
Department of Engineering Mechanics, Tsinghua University, Beijing 100084, P. R. China

(*Received* 11 *April* 1994; *in revised form* 12 *September* 1994)

Abstract—The stress–strain relation of elastic–brittle materials like concrete under tensile loading includes some of the stages of linear elasticity, pre-peak non-linear hardening, rapid stress drop and tension softening. These stages, which correspond to different mechanisms of damage, are modelled through micromechanical analyses. The behaviours of rapid stress drop and tension softening are the results of localization of damage and deformation. Based on the damage model of domain of microcrack growth proposed by Feng and Yu [*Acta Mech. Sinica* **9**, 251–260 (1993)], this paper gives the complete constitutive relation including the four stages of an elastic–brittle material subjected to uniaxial and triaxial tensile loads. As an illustration, the theoretical stress–strain curve in uniaxial tension is compared with an experimental result.

1. INTRODUCTION

Many elastic–brittle materials such as concrete, rocks and some ceramics fail through fracture preceded by countless microcracks distributed over the bulk of the material and propagating at the loading. A tensile stress–strain curve often includes the stages of linear elasticity, pre-peak non-linear hardening, tension softening etc. (Evans and Marathe, 1968). In recent years, macro- and micro-failure of materials has received wide attention. While the pre-peak response in tensile loading has been investigated relatively widely, the understanding of tension softening is still very crude.

Two main approaches are often used to investigate the constitutive relation of damaged materials. The first is the phenomenological approach based on continuum damage mechanics (Bazant and Kim, 1979; Simo and Ju, 1987; Lemaitre and Chaboche, 1988; Ortiz, 1985; Bazant and Pijaudier Cabot, 1988), in which the effects of microscopic damage mechanisms on material properties are reflected by scalar, vector or tensor damage variables. Significant advances have been made in reproducing certain portions of the macroscopic response of materials under different load histories. However, it is often difficult for these damage models to describe the complex evolution process of damage and to model the response of damaged materials subjected to complex loadings. The second approach is based on micromechanical damage mechanics, which leads to an improved understanding of the underlying physical process. In the micromechanical approach, the nucleation, growth and coalescence of microdefects are studied and their influences on mechanical properties are reflected in the constitutive relations in certain ways. Up to now, the micromechanical damage models for microcrack-weakened brittle materials reported in the open literature are mainly limited to the pre-peak non-linear hardening regime. Budiansky and O'Connell (1976), Horii and Nemat-Nasser (1983), Krajcinovic and Fonseka (1981) and some others derived the damaged compliance tensor using the self-consistent method or Taylor's model. The Mori–Tanaka method and the differential method are also two important methods to determine the stress–strain relation of damaged materials (Benveniste, 1986; Hashin, 1988).

The tension softening behaviour of brittle solids has also been considered by some authors. By introducing a unit cell containing one or more microcracks, Basista and Gross (1985) proposed a one-dimensional model to predict the quasi-plastic response of an elastic–brittle solid undergoing internal damage in uniaxial tension. Horii *et al.* (1989), Ortiz

†To whom correspondence should be addressed.

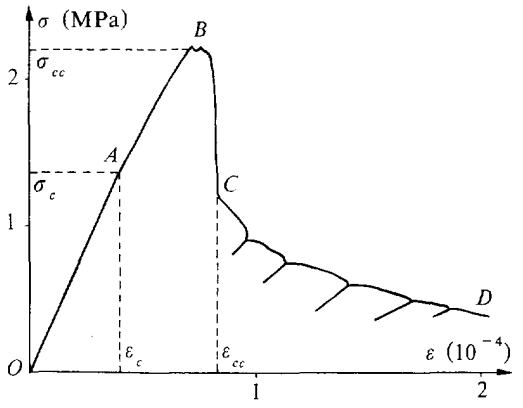

Fig. 1. A typical stress–strain curve of brittle materials in tension (Terrien, 1980).

(1988), and Huang and Karihaloo (1992) also developed several models to describe the intrinsic tension softening behaviour of quasi-brittle materials, in which discontinuous macroflaws were often treated as a series of collinear cracks subjected to normal tensile stress.

However, the micromechanisms of tension softening of brittle materials remain unclear. In fact, before tension softening occurs, complex distributed damage has evolved with the loading. The magnitudes of damage in different directions may be different and are related to the load histories. For some elastic–brittle materials, the main micromechanisms of damage are nucleation, growth and coalescence of microcracks, while other microdefects such as microvoids have no evident influence on the strength and stiffness (Luo, 1993). Feng and Yu (1993) and Yu and Feng (1995) presented a micromechanics-based damage model, in which the damage state is described by the concept of domain of microcrack growth (DMG). With the increase of applied stresses, some microcracks, having propagated along the grain boundaries and been arrested by energy barriers with higher strength, may satisfy the criterion of secondary growth and propagate further in an unstable fashion, causing a decrease of capacity of the material bearing the tensile load. The tension softening of a material is the expression of the transition from the distributed damage to the localization of damage. In this paper, the DMG damage model (Yu and Feng, 1995) is extended to the complete response of a brittle material subjected to uniaxial or triaxial tension loading. For the sake of simplicity, we do not consider the degenerative behaviour under compressive loading here; it has been discussed by Yu and Feng (1995). As an illustration, a theoretical stress–strain curve of material under uniaxial tension is given and compared with the experimental result obtained by Terrien (1980).

2. FOUR STAGES OF STRESS–STRAIN RELATION

Figure 1 demonstrates a uniaxial tensile stress–strain curve obtained experimentally by Terrien (1980) in a strain-controlled uniaxial test. This curve includes four stages, i.e. the stages of linear elasticity, pre-peak non-linear hardening, rapid stress drop and strain softening. All these stages and their corresponding damage mechanisms are analysed in the following. For the case of triaxial tensile loading, four similar stages exist, although the response of materials is more complex.

2.1. *The stage of linear elasticity (OA)*

When the tensile stress $\sigma \leqslant \sigma_c$, where σ_c is the critical stress of damage occurring, no damage occurs and no microcrack propagates in the material. All microcracks undergo only elastic deformation.

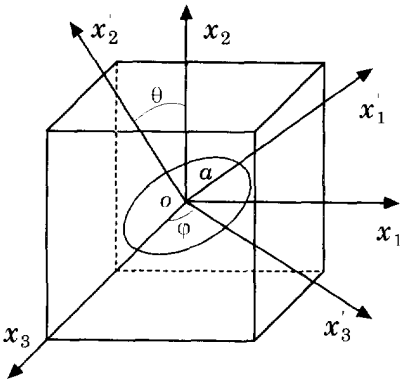

Fig. 2. A circular microcrack and the global and local coordinate systems.

2.2. *The stage of pre-peak non-linear hardening (AB)*

In the stage $\sigma_c < \sigma < \sigma_{cc}$, where σ_{cc} is the maximum stress the material can bear (Fig. 1), some microcracks grow in a stable fashion and distributed damage evolves in the material.

Consider a circular microcrack with radius a in an infinite matrix uniformly loaded at far field, as shown in Fig. 2. Establish the global coordinate system (o—$x_1x_2x_3$) and the corresponding local coordinate system (o—$x_1'x_2'x_3'$), in which x_2'-axis is parallel to the normal vector $\mathbf{n}$, and the x_3'-axis is co-planar with the x_1- and x_3-axes. The orientation of the microcrack is expressed as (θ, φ), where the two angles θ and φ are defined in Fig. 2. For such a microcrack, the growth criterion takes the form (Ju and Lee, 1991):

$$\left(\frac{K_{\mathrm{I}}'}{K_{\mathrm{IC}}}\right)^2 + \left(\frac{K_{\mathrm{II}}'}{K_{\mathrm{IIC}}}\right)^2 = 1, \tag{1}$$

where K_{I}' and K_{II}', K_{IC} and K_{IIC} are the mode I and mode II stress intensity factors (SIFs) and their critical values respectively, and

$$K_{\mathrm{I}}' = 2\sqrt{\frac{a}{\pi}}\sigma_{22}', \quad K_{\mathrm{II}}' = \frac{4}{2-\nu}\sqrt{\frac{a}{\pi}}[(\sigma_{21}')^2 + (\sigma_{23}')^2]^{1/2} \tag{2}$$

$$\sigma_{ij}'(\theta, \varphi) = g_{ik}'(\theta, \varphi) g_{jl}'(\theta, \varphi)\sigma_{kl}, \tag{3}$$

where σ_{ij} and σ_{ij}' are the stress tensors in the global and local coordinate systems respectively, and g_{ij}' are the components of the transformation matrix between the two coordinate systems (Feng and Yu, 1993):

$$g_{ij}' = \begin{bmatrix} \cos\theta\cos\varphi & \sin\theta & -\cos\theta\sin\varphi \\ -\sin\theta\cos\varphi & \cos\theta & \sin\theta\sin\varphi \\ \sin\varphi & 0 & \cos\varphi \end{bmatrix}. \tag{4}$$

Once eqn (1) is satisfied by a microcrack, it will propagate in a stable fashion, increasing its radius from the initial statistically-averaged value a_0 to the characteristic value a_u, and be arrested by grain boundaries with different directions. Then, the DMG is defined as the orientation scope of all propagated microcracks after a certain loading path. In other words, all microcracks whose normal vectors are in the orientation scope of the DMG must have propagated after the loading path.

With increasing applied stress, more microcracks satisfy the fracture criterion of a microcrack and propagate in a stable fashion. The DMG evolves and its contribution to the compliance tensor increases. So, the stress–strain relation exhibits a non-linearity. The

constitutive relations for the above two stages have been investigated by Yu and Feng (1995).

2.3. *The stage of rapid stress drop (BC)*

When the stress σ reaches the critical value σ_{cc}, some microcracks with certain orientations will satisfy the following criterion of secondary growth of a penny-shaped microcrack:

$$\left(\frac{K_{\mathrm{I}}'}{K_{\mathrm{IC}C}}\right)^2+\left(\frac{K_{\mathrm{II}}'}{K_{\mathrm{IIC}C}}\right)^2=1, \tag{5}$$

where $K_{\mathrm{IC}C}$ and $K_{\mathrm{IIC}C}$ are the critical values of SIFs describing the resistance of material against microcrack growth, which depend essentially on Δa, the change of microcrack radius. In this paper, $K_{\mathrm{IC}C}$ and $K_{\mathrm{IIC}C}$ are assumed to be material constants, while the influences of their dependence on Δa will be discussed in Section 3.4.

Once some microcracks satisfy the criterion (5), they will overcome the restriction of the grain boundaries and experience the secondary unstable growth, which may cause a transition from the distributed damage to the localization of damage and a rapid stress drop at the transition strain ε_{cc}. During this stage, only a small number of microcracks with certain orientations propagate further and other microcracks undergo elastic unloading. Under the condition of strain-controlled loading, the deformation which has received contributions from all microcracks during the first two stages concentrates gradually to the minority of microcracks experiencing the secondary growth, which results in a localization of strain. Therefore, the macroscopic stress drop is the result of the localization of damage and strain. Its basic cause is the secondary unstable growth of microcracks.

With the stress decreasing, the energy of the microcrack system decreases. After the energy reaches the minimum energy state related to the imposed macro-strain, the secondary growth of microcracks stops and then the microcrack system reaches an equilibrated state corresponding to the point C in the stress–strain curve in Fig. 1. At this point, two equations should be satisfied. One is the criterion of the secondary growth of a microcrack, the other is the equivalence between the applied strain and the sum of the strains contributed by both the matrix and all microcracks.

2.4. *The stage of tension softening (CD)*

With a further increase of imposed strain, some of the microcracks which have undergone the secondary growth will propagate further, while other microcracks will simultaneously experience unloading. At each point of CD in the curve, the two equations mentioned above should also be satisfied. Therefore, tension softening is a continuation of the damage localization and the beginning of macrocracking.

3. UNIAXIAL TENSION

In order to show the features of microscopic damage for each stage of the stress–strain relation of brittle materials, we first consider the simple case of uniaxial tension. Assume the material is subjected to uniform stress $\sigma_{ij}=0$ for $i,j=1,2,3$, except $\sigma_{22}=\sigma>0$.

3.1. *The stages of linear elasticity and pre-peak non-linear hardening*

The detailed procedure for determining the DMG and the constitutive relation for the stage of pre-peak non-linear hardening can be found in Yu and Feng (1995). In order to determine the DMG, i.e. the scope of orientation in which all microcracks have propagated under the uniaxial tension stress σ, we substitute the stress $\sigma_{22}=\sigma>0$ and $\sigma_{ij}=0$ for other indices i and j into eqns (2), (3) and the criterion (1). An equation for σ and θ is obtained as

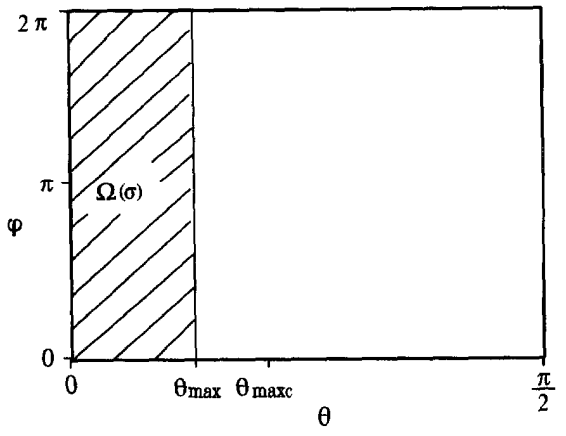

Fig. 3. The DMG under uniaxial tension.

$$\left(\frac{K_{IIC}}{K_{IC}}\right)^2 \sigma^2 \cos^4\theta + \left(\frac{2}{2-\nu}\right)^2 \sigma^2 \sin^2\theta \cos^2\theta - \frac{\pi}{4a_0} K_{IIC}^2 = 0. \tag{6}$$

The solution of this equation is

$$\tan^2\theta_{\max}(\sigma) = \begin{cases} 0 & \text{for} \quad 0 \leqslant \sigma \leqslant \sigma_c = K_{IC}\left(\dfrac{\pi}{4a_0}\right)^{1/2}, \\ \dfrac{B_2 - \sqrt{B_2^2 - 4B_1B_3}}{2B_1} & \text{for} \quad \sigma_c \leqslant \sigma \leqslant \sigma_{cc}, \end{cases} \tag{7}$$

where $\theta_{\max}(\sigma)$ is a function of the uniaxial stress σ and material data, and

$$B_1 = -\frac{\pi}{4a_0} K_{IIC}^2, \quad B_2 = \frac{\pi}{2a_0} K_{IIC}^2 - \left(\frac{2}{2-\nu}\right)^2 \sigma^2,$$

$$B_3 = \left[\left(\frac{\sigma}{K_{IC}}\right)^2 - \frac{\pi}{4a_0}\right] K_{IIC}^2. \tag{8}$$

Then the DMG of material under the condition of proportional uniaxial tension can be expressed as the set of orientation $\Omega(\sigma)$, depending on σ, in the form:

$$\Omega(\sigma) = \left\{0 \leqslant \theta \leqslant \theta_{\max}(\sigma) \leqslant \frac{\pi}{2},\ 0 \leqslant \varphi \leqslant 2\pi\right\}, \tag{9}$$

as shown in Fig. 3, which means that all microcracks with orientation $\theta \leqslant \theta_{\max}(\sigma)$ have propagated, with the final characteristic radius a_0. With increasing tensile stress σ, $\theta_{\max}(\sigma)$ increases, the DMG $\Omega(\sigma)$ grows and its contribution to the compliance tensor also increases. When σ reaches the critical stress σ_{cc} at the point B in Fig. 1, $\theta_{\max}$ reaches its maximum value $\theta_{\max c} = \theta_{\max}(\sigma_{cc})$, which is obtained from eqn (7). During the stages of rapid stress drop and tension softening, $\theta_{\max c}$ remains constant, the DMG Ω equals $\Omega(\sigma_{cc})$ and does not progress further, although some microcracks in it experience secondary growth.

Once the DMG is determined, the stress (σ_{ij})–strain (ε_{ij}) relation and the overall effective compliance tensor can be obtained as

$$\varepsilon_{ij} = S_{ijkl}\sigma_{kl}, \tag{10}$$

$$S_{ijkl} = S^0_{ijkl} + S^i_{ijkl}, \tag{11}$$

where S^0_{ijkl} is the elastic and isotropic compliance of an undamaged matrix with Young's modulus E and Poisson's ratio v, and S^i_{ijkl} is the microcrack-induced compliance tensor, which has the following form:

$$S^i_{ijkl} = \int_0^{\frac{\pi}{2}} \int_0^{2\pi} n_c p(a,\theta,\varphi)\bar{S}^i_{ijkl}(a_0,\theta,\varphi,\sigma_{ij}) \sin\theta \,\mathrm{d}\varphi \,\mathrm{d}\theta + \int_0^{\theta_{\max}} \int_0^{2\pi} n_c p(a,\theta,\varphi)[\bar{S}^i_{ijkl}(a_u,\theta,\varphi,\sigma_{ij}) - \bar{S}^i_{ijkl}(a_0,\theta,\varphi,\sigma_{ij})] \sin\theta \,\mathrm{d}\varphi \,\mathrm{d}\theta, \tag{12}$$

where n_c is the number of microcracks per unit volume of material, $p(a,\theta,\varphi)$ is the probability density function describing the distribution of the orientations and sizes of microcracks in the material, and $\bar{S}^i_{ijkl}(a,\theta,\varphi,\sigma_{ij})$ is the inelastic compliance induced by a single microcrack with radius a and orientation (θ, φ), with the form (Yu and Feng, 1993):

$$\bar{S}^i_{ijkl}(a,\theta,\varphi,\sigma_{ij}) = \frac{\pi a^3}{3} B'_{mn} g'_{2k} g'_{nl} (g'_{mi} n_j + g'_{mj} n_i) \langle \sigma_{st} g'_{2s} g'_{2t} \rangle, \tag{13}$$

where the angular brackets are defined by $\langle x \rangle = 1$ or 0 depending on whether $x \geqslant 0$ or $x < 0$, and B'_{ij} denotes the crack opening displacement tensor of the microcrack, depending upon the compliance of the microcrack-weakened material. Assuming that B'_{ij} depends only upon the compliance of the isotropic matrix, then (Ju and Lee, 1991)

$$B'_{11} = B'_{33} = \frac{16(1-v^2)}{(2-v)\pi E}, \quad B'_{22} = \frac{8(1-v^2)}{\pi E},$$
$$B'_{ij} = 0 \quad \text{for } i \neq j. \tag{14}$$

A microcrack in the material under applied stresses may be open or closed depending on its orientation and the stress tensor σ_{ij}. In this paper, only the compliances induced by open microcracks are considered; the compliances induced by closed microcracks are assumed to be zero. So, the angular brackets exist in eqn (13), and S^i_{ijkl} and $\bar{S}^i_{ijkl}$ depend upon the stress tensor σ_{ij}. For the special case of uniaxial tension, all microcracks are open and eqn (13) is simplified as

$$\bar{S}^i_{ijkl}(a,\theta,\varphi,\sigma_{ij}) = \frac{\pi a^3}{3} B'_{mn} g'_{2k} g'_{nl} (g'_{mi} n_j + g'_{mj} n_i). \tag{15}$$

In eqn (12), the probability density function $p(a,\theta,\varphi)$ satisfies the following normalization condition:

$$\int_{a_{\min}}^{a_{\max}} \int_0^{\frac{\pi}{2}} \int_0^{2\pi} p(a,\theta,\varphi) \sin\theta \,\mathrm{d}\varphi \,\mathrm{d}\theta \,\mathrm{d}a = 1, \tag{16}$$

where $a_{\max}$ and $a_{\min}$ are the maximum and minimum radii of microcracks in the material. In this paper, we assume that all microcracks are distributed uniformly in the orientation space, i.e.

$$p(a, \theta, \varphi) = \frac{1}{2\pi}. \tag{17}$$

However, in order to extend the constitutive relation obtained to more general cases, the probability density functions in eqn (12) and in the following equations are still represented as $p(a, \theta, \varphi)$.

The stress–strain relation of the first two stages of material in uniaxial tension is then obtained as

$$\varepsilon = \begin{cases} F_0\sigma, & \text{for } 0 \leqslant \sigma \leqslant \sigma_c \\ [F_0 + F_2(\theta_{\max})]\sigma, & \text{for } \sigma_c \leqslant \sigma \leqslant \sigma_{cc}, \end{cases} \tag{18}$$

where $F_2(\theta_{\max})$ is a function of σ because of the dependence of $\theta_{\max}$ on σ in eqn (7), and

$$\rho = \frac{16(1-\nu^2)n_c a_0^3}{45(2-\nu)}, \quad \gamma = \left(\frac{a_u}{a_0}\right)^3 - 1,$$

$$F_0 = \frac{1}{E} + \frac{\rho}{E}(10-3\nu),$$

$$F_2(\theta_{\max}) = \frac{\rho\gamma}{E}(10-3\nu-10\cos^3\theta_{\max}+3\nu\cos^5\theta_{\max}). \tag{19}$$

3.2. *Stress drop and tension softening*

Under higher stress, some microcracks arrested by the energy barriers, like grain boundaries, will satisfy the second growth criterion (5) and propagate in an unstable fashion, causing localization of damage, rapid stress drop and tension softening. Initially, we determine the stress σ_{cc} and the strain ε_{cc} at the transition point B. In the criterion (5), we denote

$$\bar{G} = \left(\frac{K_{\mathrm{I}}'}{K_{\mathrm{I}CC}}\right)^2 + \left(\frac{K_{\mathrm{II}}'}{K_{\mathrm{II}CC}}\right)^2. \tag{20}$$

Then the criterion (5) is written simply as

$$\bar{G} = 1. \tag{21}$$

By substituting the uniaxial tension stress into eqns (2), (3) and (20), we have

$$\bar{G} = \frac{4a_u\sigma^2\cos^2\theta}{\pi}\left[\frac{\cos^2\theta}{K_{\mathrm{I}CC}^2} + \frac{\sin^2\theta}{K_{\mathrm{II}CC}^2}\left(\frac{2}{2-\nu}\right)^2\right]. \tag{22}$$

It is easy to prove that $\partial\bar{G}/\partial\theta = 0$ and $\partial^2\bar{G}/\partial\theta^2 < 0$ when $\theta = 0$ only if $K_{\mathrm{I}CC} \leqslant \dfrac{2-\nu}{\sqrt{2}} K_{\mathrm{II}CC}$. Therefore, $\bar{G}$ reaches its maximum value,

$$\bar{G}_{\max} = \frac{4a_u\sigma_2^2}{\pi K_{\mathrm{I}CC}^2}, \tag{23}$$

at $\theta = 0$, and the microcracks normal to the tension direction will first pass through the grain boundaries and propagate in an unstable fashion. By substituting $\bar{G}_{\max}$ into eqn (21), the stress σ_{cc} is obtained as

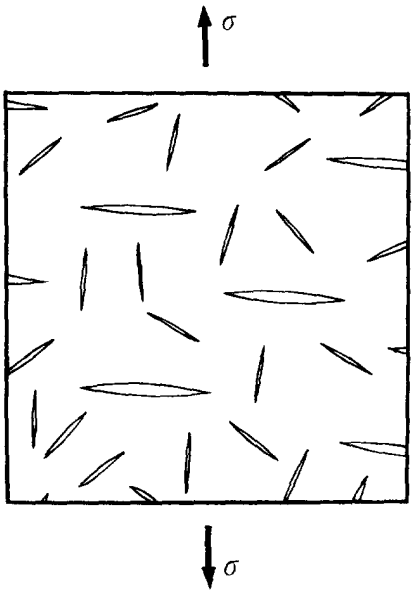

Fig. 4. The microstructure of material with microcracks experiencing secondary growth.

$$\sigma_{cc} = \frac{K_{1CC}}{2}\sqrt{\frac{\pi}{a_u}}. \tag{24}$$

From eqn (24) and the stress–strain relation (18) in the stage of pre-peak hardening, the strain at point B and during the stage of rapid stress drop (BC) is derived as

$$\varepsilon_{cc} = S_{2222}\sigma_{cc} = \frac{K_{1CC}}{2}\sqrt{\frac{\pi}{a_u}}[F_0 + F_2(\theta_{maxc})], \tag{25}$$

where $F_2(\theta_{maxc})$ is obtained from eqn (19) by replacing θ_{max} with θ_{maxc}.

After the tensile strain exceeds the threshold value ε_{cc} in eqn (25), some microcracks nearly normal to the tension direction will experience secondary growth. As mentioned above, the distribution of sizes and orientations of microcracks in the material can be described by the probability density function $p(a, \theta, \varphi)$. Then we assume that all microcracks whose orientations are within a small orientation scope $0 \leqslant \theta \leqslant \theta_{cc}$ will experience secondary growth and propagate in the material in an unstable fashion. The microscopic scenario of such a material is shown in Fig. 4. The number of microcracks experiencing secondary growth per unit volume of material is

$$n_{cc} = \int_0^{\theta_{cc}} \int_0^{2\pi} n_c p(a, \theta, \varphi) \sin\theta \, d\varphi \, d\theta. \tag{26}$$

Thus, the compliance tensor of the material during the stage of tension softening is decomposed into

$$S_{ijkl} = S^0_{ijkl} + S^I_{ijkl} = S^0_{ijkl} + S^{I1}_{ijkl} + S^{I2}_{ijkl} + S^{I3}_{ijkl}, \tag{27}$$

where S^{I1}_{ijkl} denote the components of the inelastic compliance tensor due to the microcracks with the original sizes, S^{I2}_{ijkl} denote those due to the microcracks with radius a_u and S^{I3}_{ijkl} denote those due to microcracks experiencing secondary growth. Based on the DMG damage model, we have

$$S^{t1}_{ijkl} = \int_{\theta_{max}}^{\frac{\pi}{2}} \int_0^{2\pi} n_c p(a, \theta, \varphi) \bar{S}^i_{ijkl}(a_0, \theta, \varphi, \sigma_{ij}) \sin\theta \, d\varphi \, d\theta \tag{28}$$

$$S^{t2}_{ijkl} = \int_{\theta_{cc}}^{\theta_{max}} \int_0^{2\pi} n_c p(a, \theta, \varphi) \bar{S}^i_{ijkl}(a_u, \theta, \varphi, \sigma_{ij}) \sin\theta \, d\varphi \, d\theta \tag{29}$$

$$S^{t3}_{ijkl} = \int_0^{\theta_{cc}} \int_0^{2\pi} n_c p(a, \theta, \varphi) \bar{S}^t_{ijkl}(a_s, \theta, \varphi, \sigma_{ij}) \sin\theta \, d\varphi \, d\theta, \tag{30}$$

where a_s is the radius of microcracks experiencing secondary growth, and depends on the tensile stress σ. During the stage of tension softening, the criterion (21) should be satisfied by microcracks experiencing secondary growth. Because the angle θ_{cc} is generally small, the relation between a_s and σ can be obtained approximately from the criterion (21) of secondary growth of a microcrack with orientation $\theta = 0$. For a microcrack with radius a_s and orientation $\theta = 0$, the uniaxial tensile stress gives

$$\bar{G} = \frac{4a_s\sigma^2}{\pi K^2_{ICC}}. \tag{31}$$

Substituting into eqn (21) results in

$$a_s = \frac{\pi K^2_{ICC}}{4\sigma^2}. \tag{32}$$

Thus, under the case of uniaxial tension, the complete stress–strain relation in the stage of tension softening is obtained as

$$\varepsilon = \left[F_0 + F_2(\theta_{max}) + 15\rho(2-\nu)(1-\cos\theta_{cc})\frac{1}{E}\left(\left(\frac{\pi K^2_{ICC}}{4a_0\sigma^2}\right)^3 - \gamma - 1\right)\right]\sigma, \quad \text{for } \varepsilon \geqslant \varepsilon_{cc}. \tag{33}$$

The stage of rapid stress drop intersects that of tension softening at the point C (Fig. 1). The strain at C is then equal to that at B, and the stress σ_s at C can be obtained from the following equation:

$$\left\{F_0 + F_2(\theta_{max}) + 15\rho(2-\nu)(1-\cos\theta_{cc})\frac{1}{E}\left[\left(\frac{\pi K^2_{ICC}}{4a_0\sigma_s^2}\right)^3 - \gamma - 1\right]\right\}\sigma_s = \varepsilon_{cc}. \tag{34}$$

The difference $(\sigma_{cc} - \sigma_s)$ between the stresses at B and C is the magnitude of the stress drop. Thus, the stage of rapid stress drop is also obtained.

3.3. *Comparison with experimental results*

In order to illustrate the four stages of the constitutive relation predicted by the model, the theoretical stress–strain curve in uniaxial tension given in eqns (18) and (33) is shown in Fig. 5, in which we take $K_{IC} = 0.08$ MN m$^{-3/2}$, $K_{IIC} = 0.16$ MN m$^{-3/2}$, $K_{ICC} = 0.17$ MN m$^{-3/2}$, $K_{IICC} = 0.34$ MN m$^{-3/2}$, $a_0 = 0.26$ cm, $a_u = 0.47$ cm, $E = 31{,}700$ MPa, $\nu = 0.3$, $n_c = 1.8 \times 10^6$ m^{-3} and $\theta_{cc} = 0.08$ rad. It can be shown that all of the four stages in the

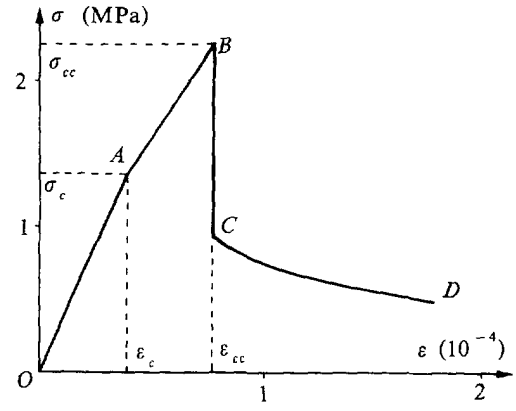

Fig. 5. The theoretical uniaxial tension stress–strain curve.

stress–strain curve in Fig. 5 are quite consistent with the experimental results of Terrien (1980) in Fig. 1. However, only the stage of tension softening in Fig. 5 is gentler than that in Fig. 1, as will be explained in the next section.

It should be mentioned that the constitutive relations (18) and (33) are obtained without considering interaction between microcracks. Such an assumption is an acceptable approximation for most stages of material before a macrocrack initiates, even though localization of damage occurs in the stage of tension softening because only a minority of microcracks experience secondary growth. If interaction between microcracks is introduced, the constitutive model will become more complicated and, of course, the results will become better.

3.4. *Effects of* K_{ICC} *and* K_{IICC}

In the discussion in other sections of this paper, K_{ICC} and K_{IICC} are simply assumed to be two material constants. However, in general, they change with the increase of microcrack radius. For different types of material considered, K_{ICC} and also K_{IICC} may be different functions of Δa describing the resistance of material against microcrack growth (Basista and Gross, 1985). Some typical shapes of the function $K_{ICC}(\Delta a)$ are shown in Fig. 6, with the various possibilities for $K_{IICC}(\Delta a)$ being similar.

The choice of the functions $K_{ICC}(\Delta a)$ and $K_{IICC}(\Delta a)$ should be based on the microstructures and properties of the materials considered. In the case of perfectly brittle materials, the SIFs K_{ICC} and K_{IICC} should not depend on the microcrack radius, i.e. $K_{ICC} = K_{I0}$ and $K_{IICC} = K_{II0}$, with K_{I0} and K_{II0} being material constants. In view of the microscopic mechanisms, the change in the internal energy due to microcrack growth is entirely contained in the surface energy. From the above discussion, we learn that the choice of K_{ICC} and K_{IICC} being two constants results in a rapid stress drop in the uniaxial tensile stress–strain curve, as shown in Fig. 5.

For some other materials, K_{ICC} and K_{IICC} should depend upon the microcrack radius. The changes of K_{ICC} and K_{IICC} with Δa are caused by the complex energy dissipative

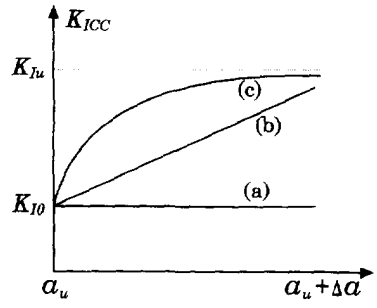

Fig. 6. Several typical forms of the function $K_{ICC}(\Delta a)$: (a) a material constant; (b) a linear function; (c) an exponential function.

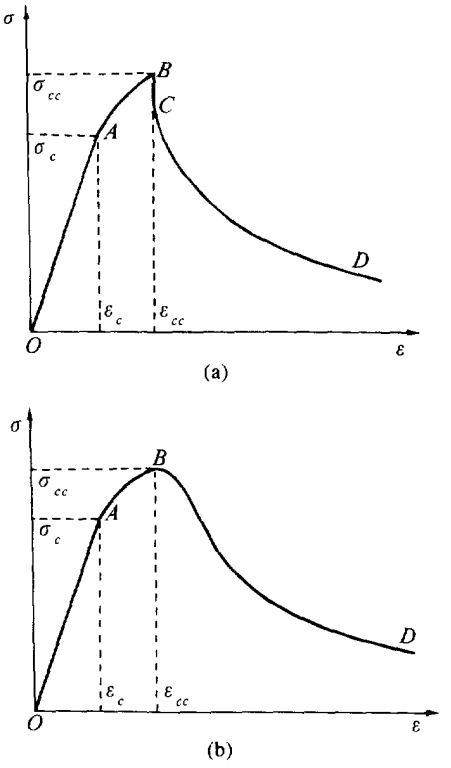

Fig. 7. The uniaxial tensile stress–strain curves for different forms of function $K_{ICC}(\Delta a)$: (a) the linear function; (b) the exponential function.

mechanism during microcrack propagation, such as the micro-plastic deformation observed even in very brittle materials and nucleation of microvoids (Basista and Gross, 1985). This conclusion was verified by experimental results reported in Broek (1974). Then, contrary to the case of idealized perfectly brittle materials, K_{ICC} and K_{IICC} are assumed to be increasing functions of Δa, such as the linear functions

$$K_{ICC} = K_{I0} + \frac{\Delta a}{a_u}\tilde{K}_I, \quad K_{IICC} = K_{II0} + \frac{\Delta a}{a_u}\tilde{K}_{II}, \tag{35}$$

and the exponential functions

$$K_{ICC} = K_{Iu} - (K_{Iu} - K_{I0}) \exp\left(-C_I \frac{\Delta a}{a_u}\right)$$

$$K_{IICC} = K_{IIu} - (K_{IIu} - K_{II0}) \exp\left(-C_{II} \frac{\Delta a}{a_u}\right), \tag{36}$$

with $\tilde{K}_I$, $\tilde{K}_{II}$, K_{Iu}, K_{IIu}, C_I and C_{II} all being material constants (Basista and Gross, 1985), as shown in Fig. 6. When the linear functions (35) are adopted, the analysis of the stress–strain relation is similar to that in Section 3.2. The stress–strain curve in the stage of tension softening will become steeper, and the magnitude of sudden stress drop will become smaller and even disappear for bigger $\tilde{K}_I$ and $\tilde{K}_{II}$, as shown in Fig. 7(a).

When the exponential functions (36) are used, the shape of the uniaxial tensile stress–strain curve changes further. The stage of rapid stress drop cannot be observed for general material constants. A corresponding stress–strain curve is shown in Fig. 7(b).

4. TRIAXIAL TENSION

For simplicity, the general three-dimensional stress is first transformed into the principal stress coordinate system, and we let the global coordinate system be consistent with the principal stress coordinate system. Therefore, in the global coordinate system (o—$x_1x_2x_3$) in Fig. 2, the components of stresses tensor are $\sigma_{11}=\sigma_1$, $\sigma_{22}=\sigma_2$, $\sigma_{33}=\sigma_3$ and $\sigma_{ij}=0$ for $i\neq j$, in which σ_2 is assumed to be the maximum principal stress.

4.1. *Orientation of microcracks undergoing secondary growth*

Substituting the triaxial tensile stress in the principal stress coordinate system into eqns (2), (3) and (20) leads to

$$\bar{G}=\frac{4a_u}{\pi K_{\mathrm{I}CC}^2}(\sigma_1\sin^2\theta\cos^2\varphi+\sigma_2\cos^2\theta+\sigma_3\sin^2\theta\sin^2\varphi)^2+\frac{4a_u\sin^2\theta}{\pi K_{\mathrm{II}CC}^2}\left(\frac{2}{2-\nu}\right)^2$$
$$[\cos^2\theta(\sigma_2-\sigma_1\cos^2\varphi-\sigma_3\sin^2\theta)^2+\sin^2\varphi\cos^2\varphi(\sigma_1-\sigma_3)^2]. \quad (37)$$

We can prove that, provided that

$$K_{\mathrm{I}CC}\leqslant\frac{2-\nu}{\sqrt{2}}K_{\mathrm{II}CC},$$

$\bar{G}$ reaches its maximum value $\bar{G}_{\max}$ in the same form as eqn (23) when $\theta=0$. Therefore, for the case of triaxial tension, the microcracks normal to the maximum principal stress will first undergo secondary growth. From $\bar{G}_{\max}=1$, the condition of rapid stress drop can also be obtained as

$$\sigma_2=\sigma_{cc}=\frac{K_{\mathrm{I}CC}}{2}\sqrt{\frac{\pi}{a_u}}, \quad (38)$$

which shows that the transition point is related only to the maximum principal stress, but not the two others.

4.2. *Constitutive relation*

Under the condition of proportional stress loading, when the maximum principal stress $\sigma_2<\sigma_c$, the stress–strain relation is isotropic and linear elastic, and

$$\varepsilon_{ij}=(S^0_{ijkl}+S^{i1}_{ijkl})\sigma_{kl}, \quad (39)$$

where

$$S^{i1}_{ijkl}=\int_0^{\frac{\pi}{2}}\int_0^{2\pi}n_c p(a,\theta,\varphi)\bar{S}^i_{ijkl}(a_0,\theta,\varphi,\sigma_{ij})\sin\theta\,\mathrm{d}\varphi\,\mathrm{d}\theta. \quad (40)$$

When $\sigma_c\leqslant\sigma_2<\sigma_{cc}$, the DMG Ω can be calculated by substituting the stress tensor σ_{ij} into the criterion (1) (Yu and Feng, 1995). The stress–strain relation in this stage is anisotropic and non-linear:

$$\varepsilon_{ij}=(S^0_{ijkl}+S^{i1}_{ijkl}+S^{i2}_{ijkl})\sigma_{kl}, \quad (41)$$

where

$$S^{i1}_{ijkl} = \int_0^{\frac{\pi}{2}} \int_0^{2\pi} n_c p(a, \theta, \varphi) \bar{S}^i_{ijkl}(a_0, \theta, \varphi, \sigma_{ij}) \sin\theta \, d\varphi \, d\theta$$

$$- \iint_{\Omega} n_c p(a, \theta, \varphi) \bar{S}^i_{ijkl}(a_0, \theta, \varphi, \sigma_{ij}) \sin\theta \, d\varphi \, d\theta \quad (42)$$

$$S^{i2}_{ijkl} = \iint_{\Omega} n_c p(a, \theta, \varphi) \bar{S}^i_{ijkl}(a_{ii}, \theta, \varphi, \sigma_{ij}) \sin\theta \, d\varphi \, d\theta. \quad (43)$$

Once σ_2 reaches σ_{cc}, the stress will drop rapidly. The strains ε_{ccij} at the transition point can be obtained from eqn (41) by using $\sigma_{22} = \sigma_{cc}$ and the condition of proportional stress loading. The changing paths of stresses and strains after the transition point depend on the mode of loading. For the case of stress-controlled loading, the microcrack will propagate continuously until macroscopic failure occurs in the material, and the stage of gentle tension softening cannot be observed. Here, we assume the maximum principal strain ε_{22} is controlled to increase very slowly while all the components of the stress tensor change in the original proportions. Then, after a certain magnitude of stress drop, the rapid stress drop will stop and the material will exhibit tension softening behaviour. At any time of tension softening, two equations must be satisfied. The first is the criterion of secondary growth of microcracks, which gives the relation between the microcrack radius a_i and the stress σ_{ij} in similar form to eqn (32) by replacing σ with σ_2. The second is based on the equivalence between the imposed strain and the sum of strains contributed by both matrix and all microcracks; the constitutive relation for the stage of tension softening is then

$$\varepsilon_{ij} = (S^0_{ijkl} + S^{i1}_{ijkl} + S^{i2}_{ijkl} + S^{i3}_{ijkl})\sigma_{kl}, \quad (44)$$

where S^{i1}_{ijkl} and S^{i3}_{ijkl} are same as eqns (42) and (30), and

$$S^{i2}_{ijkl} = \iint_{\Omega} n_c p(a, \theta, \varphi) \bar{S}^i_{ijkl}(a_{ii}, \theta, \varphi, \sigma_{ij}) \sin\theta \, d\varphi \, d\theta$$

$$- \int_0^{\theta_{cc}} \int_0^{2\pi} n_c p(a, \theta, \varphi) \bar{S}^i_{ijkl}(a_{ii}, \theta, \varphi, \sigma_{ij}) \sin\theta \, d\varphi \, d\theta. \quad (45)$$

The intersection point between the stage of rapid stress drop and tension softening, and also the magnitude of stress drop can be obtained from eqn (44) and $\varepsilon_{22} = \varepsilon_{cc22}$. So the complete constitutive response of an elastic–brittle material under triaxial tension under the condition of proportional loading is obtained.

5. CONCLUSIONS

In this paper a micromechanics-based model has been proposed for elastic–brittle materials undergoing irreversible changes of their microscopic structures due to microcrack growth.

The basic idea of the present model is to classify the constitutive relation of brittle materials into four stages and to investigate their corresponding microcrack damage mechanisms individually. In the stage of pre-peak non-linear hardening, the distributed damage due to the stable propagation of microcracks can be described by the concept of DMG suggested by Feng and Yu (1993). After the applied stress exceeds the bearing capacity of the material, localization of damage and strain occurs, which causes a sudden rapid stress drop and tension softening behaviour of the material. The influences of all microcracks with different sizes and orientations are introduced into the overall compliance tensor by

using the statistical average method based upon Taylor's model. Although only the case of proportional loading is investigated, it is possible to extend the theory to the problems of complex loading by using a procedure similar to that given by Yu and Feng (1995).

However, it should be pointed out that some other factors still have to be considered. To this end the effects of microcrack interaction may be introduced by the self-consistent method. The damage-related residual strain in unloading should also be mentioned, even for some brittle materials.

Acknowledgements—This work was supported by the Doctoral Program Foundation of the State Education Committee and the National Natural Science Foundation of China. The authors thank Prof. Dr-Ing D. Gross for helpful discussions.

REFERENCES

Basista, M. and Gross, D. (1985). One-dimensional constitutive model of microcracked elastic solid. *Arch. Mech.* **37**, 587–601.

Bazant, Z. P. and Kim, S. S. (1979). Plastic-fracturing theory for concrete. *J. Engng Mech. ASCE* **115**, 407–428.

Bazant, Z. P. and Pijaudier Cabot, G. (1988). Nonlocal continuum damage, localization, instability and convergence. *J. Appl. Mech.* **55**, 287–293.

Benveniste, Y. (1986). On the Mori–Tanaka's method in cracked solids. *Mech. Res. Commun.* **13**, 193–201.

Brock, D. (1974). *Elementary Engineering Fracture Mechanics*. Sijthoff & Noordhoff, The Netherlands.

Budiansky, B. and O'Connell, R. J. (1976). Elastic moduli of a cracked solids. *Int. J. Solids Structures* **12**, 81–97.

Evans, R. H. and Marathe, M. S. (1968). Microcracking and stress–strain curves for concrete in tension. *Matér. Construct.* **1**, 61–64.

Feng, X. Q. and Yu, S. W. (1993). A new damage model for microcrack-weakened brittle materials. *Acta Mech. Sinica* **9**, 251–260.

Hashin, Z. (1988). The differential scheme and its application to cracked materials. *J. Mech. Phys. Solids* **36**, 719–734.

Horii, H., Hasegawa, A. and Nishino, F. (1989). Fracture process and bridging zone model and influencing fracture of concrete. In *Fracture of Concrete and Rock* (Edited by S. Shah and S. Swartz), pp. 205–209. Springer, New York.

Horii, H. and Nemat-Nasser, S. (1983). Overall moduli of solids with microcracks: load-induced anisotropy. *J. Mech. Phys. Solids* **31**, 155–171.

Huang, X. and Karihaloo, B. L. (1992). Tension softening of quasi-brittle materials modelled by single and doubly periodic arrays of coplanar penny-shaped cracks. *Mech. Mater.* **13**, 257–275.

Ju, J. W. and Lee, X. (1991). Micromechanical damage models for brittle solids. I. The tensile loadings. *J. Engng Mech. ASCE* **117**, 1495–1514.

Krajcinovic, D. and Fonseka, G. U. (1981). The continuous damage theory of brittle materials. *J. Appl. Mech.* **48**, 809–824.

Lemaitre, J. and Chaboche, J. L. (1988). *Mechanics of Material Solids*. Cambridge University Press, London.

Luo, Y. Q. (1993). Investigation on Micromechanisms of Damage in Cement Paste. Thesis of Master Degree, Neimonggu College of Technology.

Ortiz, M. (1985). A constitutive theory for the inelastic behavior of concrete. *Mech. Mater.* **4**, 67–93.

Ortiz, M. (1988). Microcrack coalescence and macroscopic crack initiation in brittle solids. *Int. J. Solids Structures* **24**, 231–250.

Simo, J. C. and Ju, J. W. (1987). Strain- and stress-based continuum damage models—I. Formulation. *Int. J. Solids Structures* **23**, 821–840.

Terrien, M. (1980). Emission acoustiqueet comportment post-critique d'un béton sollicitéen traction. *Bull. Liaison Ponts Chaussées* **105**, 65–72.

Yu, S. W. and Feng, X. Q. (1995). A micromechanical-based damage theory for microcrack-weakened brittle solids. *Mech. Mater.* (in press).